

Received September 7, 2017; reviewed; accepted March 20, 2018

Mechanisms for the improved flotation of inherently hydrophobic graphite in electrolyte solution

Qingteng Lai ¹, Yinfei Liao ², Zechen Liu ¹, Yucheng He ¹, Yifan Zhao ¹

¹ China University of Mining and Technology, Key Laboratory of Coal Processing and Efficient Utilization of Ministry of Education, 221116, Jiangsu, China

² China University of Mineral and Technology, 221116, Jiangsu, China

Corresponding author: 1039144004@qq.com (Yinfei Liao)

Abstract: It is well documented that unavoidable ions in a pulp such as Mg²⁺, Ca²⁺, and K⁺ have a significant effect on the interaction for particles, especially for flotation of metallic sulfide minerals and clay minerals. In this study, the effect of electrolytes on the flotation of inherently hydrophobic mineral-graphite was studied. It was found that the zeta potential showed a dramatic decrease, and the reagent adsorption capacity of mineral enhanced in the present of electrolytes. The possible mechanism responsible for improved recovery was investigated by electrokinetic, surface tension and ions adsorption tests. It is likely that the hydrophobic force is stronger than the electrostatic force due to the reduced potential of graphite. This might be in favor of the formation of hydrophobic oil film leading to an increase in the graphite floatability. The experiments provided a new spectacle to study inherently hydrophobic mineral processing with electrolyte solution.

Keywords: flotation, electrolyte, low-grade, graphite

1. Introduction

With the depletion of high-grade ores and sustainable growth in demand by society for graphite, more and more highly disseminated, low-grade ores are processed. The sufficient deliberation of low-grade minerals requires fine grinding, which will reduce the separation efficiency and increase the loss of valuable minerals (Pease et al., 2006; Xing et al., 2017). Thorough knowledge about the graphite material, it is reasonable to know that the decreasing particle size would result in an increased exposure rate of covalent bond in layer. Therefore, fine graphite particles show a higher affinity to surrounding liquid due to its greater unsaturated bond energy. Moreover, this poses a challenge for the separation of low-grade and fine dissemination size graphite ore. Besides, with the particle size decreasing, the radius of curvature (Lee et al., 2005), and the specific surface area are increasing, which also leading to a greater metallic solubility of minerals in pulp. Therefore, some unavoidable metal ions are present within the pulp, especially for recycled water. In addition, as a result of the scarcity of fresh water and increasingly crucial environment protection, in the past decades, many plants have done processing practice in high ionic strength aqueous such as seawater (Dickson and Goyet, 1994; Liu and Peng, 2014; Hirajima et al., 2016), underground water, and re-used water.

Flotation of ultra-fine particles and their separation from gangue minerals are contrasting in deionized water and electrolytes solution (Wang et al., 2014). The mechanism of action is analyzed from two aspects: Bubble or particle itself, where a variety of probable mechanisms as inhibition of bubble coalescence, stabilizing the froth layer, compression electric double layer, and destabilization of the hydrated layer are proposed. Paulson and Pugh (1996) reviewed the effect of electrolytes on the flotation of graphite. Electrolytes would degrade dissolved gas concentration gradients in pulp and further inhibit the bubble coalescence. The increased recovery was contributed to an increase in the collision probability with higher concentration of smaller non-coalescing bubbles. The similar inhibition of

bubble coalescence was also observed in Graig's experiment (Craig et al., 1993). Besides, electrolytes have an ability to enhance second beneficiation through further stabilizing the froth layer (Castro and Laskowski, 2011; Manono et al., 2012). As reported by Ozdemir (2013), the bubble coalescence was inhibited significantly in the presence of some salts such as NaCl, KCl, and MgCl₂, which contributed to the increase in recovery. However, the ash content was also increased due to the entrainment of the gangue minerals. The copper ions in the flotation pulp could activate the chalcopyrite as a result of the interactions between copper ions and sulfur on the chalcopyrite surface (Zhao and Peng, 2012). This adsorption increased the flotation rate, and hence the improvement of recovery.

Bentonite is a common clay mineral with a formation of phyllosilicate minerals comprising silica tetrahedral sheets and alumina octahedral sheets in flotation. The presence of bentonite would increase the pulp viscosity, resulting in a decrease in bubble-particle collision efficiency. The addition of cations reduced the yield stress drastically, which was beneficial to the improvement of recovery (Lagaly and Ziesmer, 2003; Liu and Peng, 2014; Wang et al., 2016). As reported by Rattanakawin and Hogg (2001) and Liang et al. (2007), electrolytes compressed electrical double layers, and therefore, reduced the detriment electrostatic adsorption between particles. Peng and Bradshaw (2012) demonstrated that pentlandite flotation in the presence of lizardite was improved in saline water due to the compression of electrical double layers. Zhao (2016) investigated the mitigation of clay slime coating on chalcocite by impedance spectroscopy in the presence of electrolytes. The results demonstrated that the electrolytes could reduce the electrostatic attraction between chalcocite and clay particles. However, the addition of sodium silicate and sodium hexametaphosphate did not enhance the flotation recovery significantly in the study of Oats et al. (2010), which is probably due to that double-layer interaction played a secondary role while van der Waals attraction played a main role. The addition of Ca²⁺ reduced electrostatic repulsion between kaolinite particles, which induced an increase in settling rate allowing effective separation of valuable and gangue minerals (Gui et al., 2016). Choi (2016) found that Na⁺ ions effectively screen a negatively charged bubble surface, reducing the energy barrier for attachment and thus increasing floatability. The increased floatability is well explained by the extended DLVO theory. Manono (2016) contributed the effect of electrolyte on flotation to the motivation that related to the gangue minerals. Hancer (2001) proposed that the ions through the electrolyte aqueous might destabilize the formation of water film around particles, and this is beneficial to reagent adsorption. The unstable hydration film was easy to rupture so as to form bubble-particle attachment (Pan and Yoon, 2016). Overall, fundamental studies and plant operations mentioned above have clearly shown that ionic strength of pulp had significant effects on the recovery of valuable minerals, especially for fine particles.

The purpose of this study was to further understand how the electrolytes, namely MgCl₂, KCl, and MgSO₄, affect the flotation behavior of inherently hydrophobic mineral graphite. Additionally, the effect of Mg²⁺ ions on zeta potential of particles and surface tension of water at various MgCl₂ concentrations was investigated. Finally, the adsorption experiments of Mg²⁺ on graphite surface was carried by ICP.

2. Experimental

2.1 Materials and reagents

Graphite ore used in this study was obtained from Jixi (Heilongjiang, China), which was crushed through a jaw crusher and a hammer crusher to obtain -2 mm particle size. The crushed products were ground at 50% solid ratio in tap water using a laboratory scale stainless steel rod mill to achieve the grinding product of 95.34% passing 74 μm. The fixed carbon content of sample was measured by automatic industrial analyzer (5E-MAG6700 II, China). The results showed that the fixed carbon content was 10.06%, which indicated that the graphite was low-grade ore. The sample used for the experiments (Zeta potential measurement, surface tension, FTIR measurement, measurement of adsorption capacity) was graphite ore, not pure graphite.

Diesel and pine oil (industrial grade) were used as a collector and frother, respectively. Other chemicals used in this study were analytical reagent.

2.2 Methods

2.2.1 Materials characterization

The XRD (X-Ray Diffraction, D8 Advance, German) analysis was used to determine the mineral composition of the sample. Analysis of element content in gangue minerals was conducted using XRF (X-Ray Fluorite Spectroscopy S8 Tiger, Germany). The morphological characteristics and gangue distribution of the samples were investigated by FEI Quanta™ 250 (USA) scanning electron microscope. The sample was dried in an oven (below 50°C), then it was uniformly attached to the sample plate. And, the attached sample was adequately dispersed to ensure that no overlap occurred. After that, the sample was plated with gold due to the low conductivity. Deionized water (resistivity is 12 MΩ.cm.) (Provided by Sida Technology Corporation, China) and pure gold powder (Less than 10 nm) were used for the experiments.

2.2.2 Flotation

Flotation tests were conducted using a 1.5 dm³ Denver flotation cell with air flow rate of 0.1 m³/h at the pH of 7. For the flotation, 225 g of ground sample was first added into the tank and mixed with 1.5 dm³ tap water. The solid ratio of the pulp was about 15%. Then, the pulp was conditioned at 2100 rpm until the graphite sample was wetted fully. The collector (2200 g/Mg) was added, and conditioned for 3 min, and the frother (400 g/Mg) was added into the slurry, and stirred for another period of 2 min. The optimum reagent dosage was determined by comparison of the fixed carbon content and recovery rate of concentrate in the flotation tests. The amount of collector used for the reagent exploration tests were 1600, 1800, 2000, 2200, and 2400 g/Mg while the dosage of frother were 200, 300, 400, 500, and 600 g/Mg respectively. Besides, the flotation was carried out for 9 min. After completion of the flotation, the rougher concentrate and tailing were collected, and removed most of the water through a vacuum filter (CTDL5C-φ240/φ120 disc vacuum filter), and were further dried in an oven (below 50°C), then weighed. The fixed carbon of flotation products was analyzed by automatic industrial analyzer (5E-MAG6700).

2.3.3 Zeta potential measurements

Zeta potential measurement of graphite sample in the absence and presence of electrolytes was conducted by ZetaPALS+ZTU Potential Analyzer (USA) which calculates the zeta potential of the particles from the measurement of electrophoretic mobility using electrophoresis. Mixed 0.05 g of graphite with 100 cm³ DI water and desired amount of electrolytes were added into the suspension. After that, the prepared suspension was conditioned using a magnetic stirrer for 10 min, and then left to stand for 10 h. The concentrations of the electrolytes were 0, 0.05, 0.1, 0.2, 0.3 mol/dm³. The supernatant of settled solution, of the order of 0.1% solids by mass, was taken to measure the electrophoretic mobility, which was carried out at 25 °C and pH 7. In each test, the presented results were the average of five independent measurements. The average error of measurements was 0.021.

2.3.4 Adsorption experiments

A 10 g of graphite ore sample was added into a 250 cm³ beaker and conditioned with 0.3 mol/dm³ MgCl₂ solution for 30 min. The particle size of each sample was determined by Laser particle size analyzer (S3500, USA), and the results are presented in Table 2. After stand for 10 h, the supernatant of the mixture was taken for the measurement of ion concentration using optima 8300 (China). The electron produced by argon ionization in the electric field and magnetic field was used to bombard the sample, the resulting the energy transition of the elements in the sample and hence the formation of characteristic spectral lines. The adsorption amount of Mg²⁺ on graphite surfaces was calculated according to the balance Eq. 1.

$$Q_t = \frac{(C_i - C_r) \cdot V}{M} \quad (1)$$

where Q_t is the adsorption amount of Mg²⁺ on graphite surfaces at time t (mol/g), C_i is the initial concentration of Mg²⁺ (mol/dm³), C_r is the equilibrium concentration of Mg²⁺ (mol/dm³), V is the slurry volume (dm³), and m is the mass of graphite (g).

2.3.5 FTIR measurements

The measurement of FTIR was conducted using the traditional potassium bromide squash method. Before the test, potassium bromide was dried sufficiently in an infrared drying oven. Then, the graphite and potassium borate were mixed in proportion to 1:150 (wt/wt). The obtained mixture was made into a tablet for the examination using Fourier Transform Infrared Spectroscopy Vertex 80v (Germany). And, the FTIR spectra were recorded in the range of 400 cm^{-1} to 4000 cm^{-1} .

2.3.6 Surface tension experiments

Surface tension measurement was carried out with a K100 (KRUSS company). Firstly, 10 g of graphite was mixed with 100 cm^3 deionized water at a speed of 800 rpm until the graphite was fully wetted. Then, a desired amount of MgCl_2 electrolytes was added into the slurry and stirred for 15 min, after which diesel (collector, 2200 g/Mg) was added and continue stirring for 30 min. Finally, the prepared suspension was settled for 4 h. The upper liquid was transferred into the cell for the surface tension measurement to determine the effect of electrolytes on the adsorption capacity of collector on graphite particle surface. Since K100 can only be used to measure the gas-liquid interfacial tension, the amount of collector on the particle surface cannot be measured directly. However, the amount of adsorption can be indirectly characterized by the residual amount of collector in the upper liquid.

3. Results and discussion

3.1 Characterization of materials

As can be seen from X-ray diffraction patterns (Fig. 1), the ore contained quartz and gismondine as the main gangue minerals and graphite as valuable minerals. The results for element composition of the gangue determined by XRF (X-Ray Fluorite Spectroscopy S8 Tiger, Germany) is presented in Table 1, where the high levels of Si in the results of XRF analysis was due to the presence of large amounts of quartz. Similarly, gismondine contribute to the high content of Ca and Al.

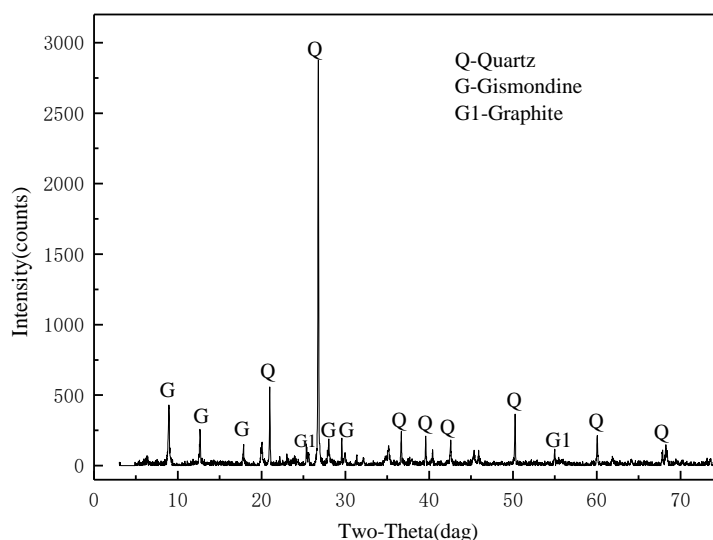


Fig. 1. X-ray diffraction (XRD) patterns of graphite ore

The element of Fe is the component of lizardite. However, the peak of the lizardite was not marked in the XRD patterns due to the low content of the lizardite in the graphite ore. For gangue minerals, the sum of mass fraction for Si, Al, and Ca in crude graphite detected by the XRF analysis were 94.90%. Combined with the XRD analysis, the major components of sample were obtained as quartz and graphite. Therefore, the beneficiation process was mainly to solve the separation of quartz, gismondine and graphite. The element mapping for C, O, Si, Al, and Fe detected by SEM-EDS (FEI QuantaTM 250, USA) analysis is shown in Fig. 2. The widespread distribution of the elements of O, Si, and C indicated the fine dissemination relationship between graphite and quartz, which posed a processing challenge.

Table 1. Element composition (wt%) of gangue of flotation sample

Elements	Ga	As	K	Sr	Zn	Rb	Br	Zr	Mn
Percentage (wt%)	0.0051	0.0051	0.0080	0.0164	0.0182	0.0288	0.0393	0.0503	0.0604
Elements	Ba	S	Mg	Ti	Fe	Na	Ca	Al	Si
Percentage (wt%)	0.1695	0.1803	0.5677	0.9453	1.1376	1.8547	8.2400	18.3755	68.2975

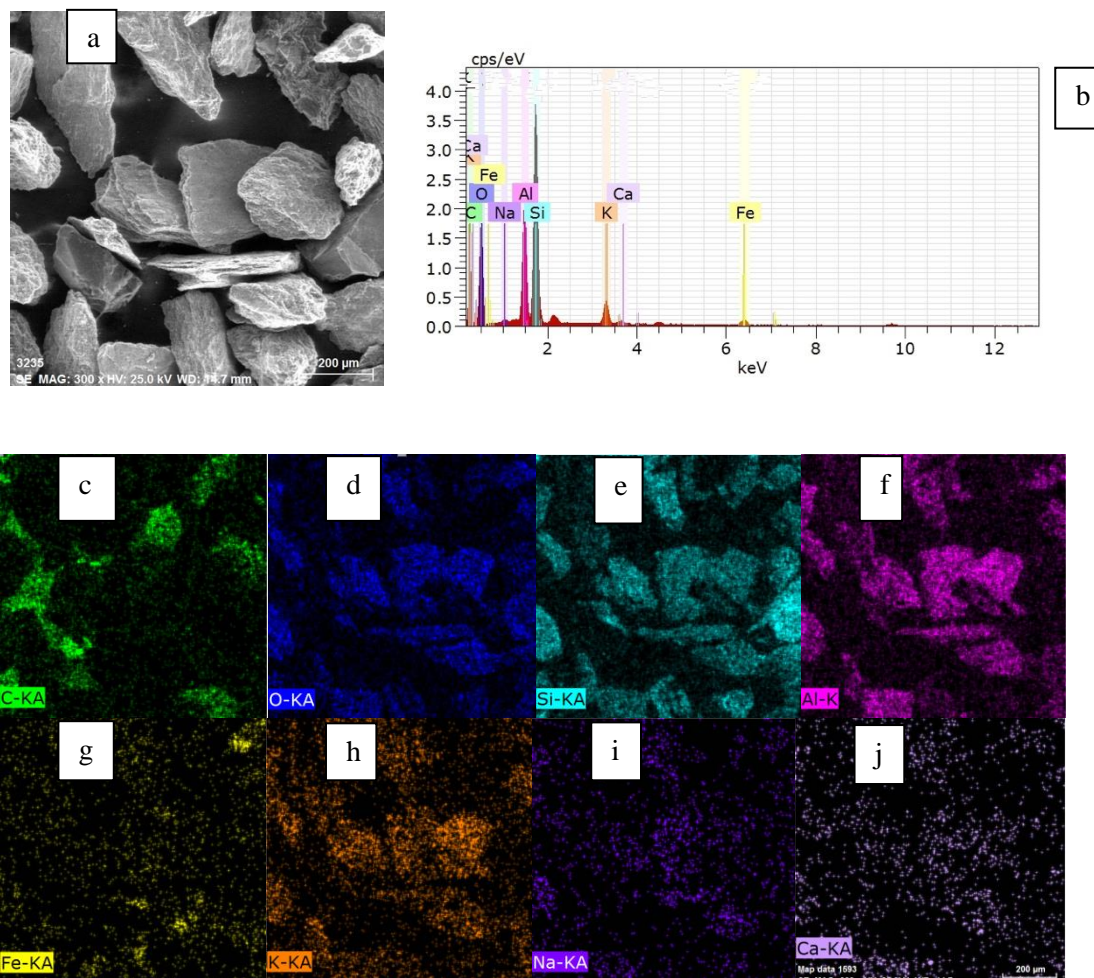


Fig. 2. SEM-EDS analysis of raw graphite sample (a) surface morphology of the sample (b) elemental composition of the sample (c, d, e, f, g, h, i, j) distribution of C, O, Si, Al, Fe, K, Na, and Ca elements in the sample respectively

3.2 Flotation results

The effect of electrolytes on the flotation process was investigated for each electrolyte. The results seen in Fig. 3 showed that upon KCl addition, the recovery of graphite markedly increased from a blank test recovery of 85.62% (no electrolyte) to 89.15% with a little increase in fixed carbon content of concentrate. The maximum recovery of graphite was obtained as 91.26% with the addition of MgSO_4 . Besides, the recovery of graphite was 91.12% in the presence of MgCl_2 . The flotation results indicated that the electrolytes not only increased graphite recovery but also had a little contribution to the upgrade of concentrate. This might be associated with the reducing interaction between graphite and gangue minerals, which greatly promoted the dispersion of minerals. The dispersed graphite particle without the attachment of hydrophilic gangue minerals had a better hydrophobicity, and then were easily captured by the oily collector. Therefore, the addition of electrolytes led to an increase in the graphite recovery. As the better separation of graphite from gangue minerals, the entrainment was weakened reducing the impurities content of concentrate. Another mechanism reported by (Klassen and Mokrousov, 1963) is that the inorganic electrolytes destabilized the hydrated layers surrounding

particles and reduced their surface hydration therefore enhancing the bubble-particle attachment. Besides, Mishchuk (2005) and Zhang and Ducker (2007) proposed the formation of small bubbles on coal surfaces in electrolyte solutions were attributed to the increased bubble-coal attachment, and therefore coal flotation.

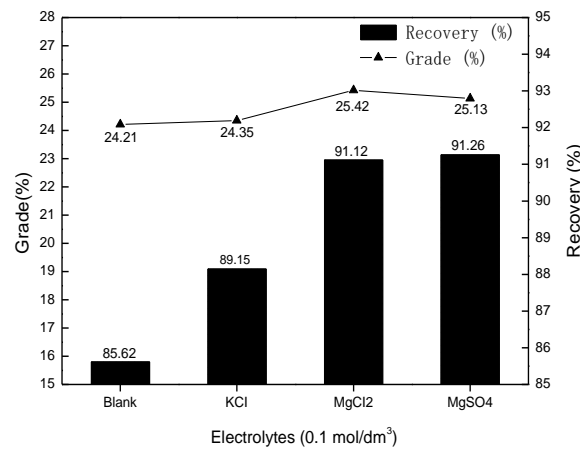


Fig. 3. Effect of electrolytes on the flotation recovery and concentrate grade of graphite

3.3 Zeta potential measurements

Figure 4 shows the zeta potential of graphite as a function of electrolytes concentration at pH=7. The zeta potentials of sample were negative over all electrolytes concentration gradient from 0 mol/dm³ to 0.1 mol/dm³ in both MgCl₂ and KCl solutions. And, both of electrolytes-zeta potential curves showed a decrease in the magnitude of zeta potential with the increasing of ionic strength. However, the potential in KCl solution was more negative than that of in MgCl₂ solution at the same concentration condition. This was probably due to high valence ions that have a stronger ability of compressing electric double layer. Electrostatic repulsion was reduced with the addition of electrolytes, which was also reported elsewhere (Ozdemir et al., 2009). As seen in Fig. 4, the change of zeta potential value of graphite was closely related to the valence and concentration of electrolytes, which is in accordance with the study of Paulson and Pugh (1996). This decrease in the zeta potential which resulted in the increase of mineral recovery was probably due to the reduced electrostatic attraction between graphite and gangue and the improved attachment of collector. The relationship between reduced charge and floatability was further investigated through measurement of surface tension.

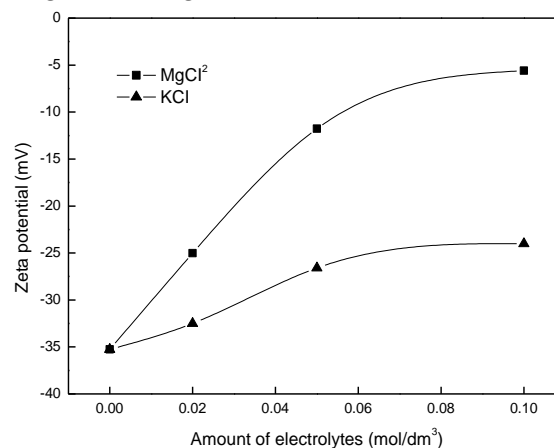


Fig. 4. Effect of electrolytes on the potential of graphite

The measurement of zeta potential and other studies about electrolytes mentioned in introduction section clearly indicated that the cations have an effect on compressing electrical double layer. The similar results were also observed in the study of Li and Somasundaran (1991). There are two causes for this decrease in zeta potential. On the one hand, the increased opposite charged ions would induce a

decrease of electrokinetic potential. On the other hand, ions adsorbed on the stern layer of electric double layer also causes a similar decrease of electrokinetic potential (Crundwell, 2016). However, previous literature related to compressed double layer did not identify the specific cause of decreased zeta potential which is the increased opposite charged ions or both of high concentration of opposite charged ions and adsorption of ions on the stern layer.

3.4 Adsorption experiments

Adsorption capacity is closely related to the particle size at the constant conditions. Ions can be more easily adsorbed by fine particles due to the high surface energy and large surface area (Chen and Peng, 2015). Therefore, the adsorption capacity will have a difference in the adsorption tests of various particle sizes if ions adsorption dose exit. Detailed particle size information of the three particle size fractions that was used for adsorption experiment is presented in Table 2.

Table 2. Particle size composition of adsorption test samples (passing %)

Particle size (μm)	250	125	74	45	38	19	10	5.5
a*	100	98.1	90.42	71.66	64	40.3	29.16	20.31
b*	100	100	98.86	92.79	88.34	61.98	45.67	35.48
c*	100	100	98.53	94.33	91.45	74.72	62.47	49.97

*a, b, and c represent coarse, medium, and fine sizes of particles, respectively

Table 3. Results for adsorption experiments

Sample	Ion concentration of supernatant (10^{-5} mol/dm^3)	Adsorption capacity (The mass ratio of electrolytes to graphite) ($\mu\text{g/g}$)
a	4.38	44.30
b	4.35	47.25
c	4.15	66.40
Blank	4.85	--

It can be seen clearly from Table 3 that the concentration of MgCl_2 ions with coarse particles was significantly higher than that of fine particles in the supernatant. This indicated that part of ions adsorbed on the surface of graphite ore in pulp. The adsorption capacity showed an increase with the decreasing of particle size. Therefore, not only ions adsorption but also increased concentration of opposite charged ions in the solution worked for the compression of double electric layer.

The isoelectric point of graphite is between 2 and 3 (Rath and Laskowski, 1999). Therefore, the charge of graphite is negative in weakly acidic or non-acid pulp. Gismondine, impurity of the graphite ore, is positive charge due to the better ion exchange property. The compressing action of electrolytes on double layer of mineral would weaken the electrostatic attraction of graphite and gismondine. Thus, the reduction of potential favors the interaction between graphite and collector, and hence the recovery of graphite. Furthermore, Wang and Peng (2013) found that saline water enhanced the aggregation of fine particles resulting in the increased recovery of minerals.

3.5 FTIR analysis

The FTIR measurement was carried out to further determine the adsorption type and adsorption capacity. The results of FTIR are shown in Fig. 5. Vibrations related to internal Si-O(Si) and Si-O(Al) bonds is in the range $1200\text{--}400 \text{ cm}^{-1}$. The peak at 797 cm^{-1} is characteristic of the quartz which belongs to gangue mineral, and the presence of this peak is due to the Si-O-Si symmetrical stretching vibration. This was further illustrated by the low transmittance of mineral Si-O-Si and Si-O-Al at 1032 cm^{-1} . Based on the XRD analysis, Si-O-Si is the composition of quartz and Si-O-Al is representative component of gismondine. The peak appearing at around 1425 cm^{-1} is related to $-\text{CH}_2$ and CH_3 . As can be seen from

the spectra, the surface area above the peak appeared at 1425 cm^{-1} with electrolytes is less than that of the sample without the addition of electrolytes. It suggested that the adsorption density of collector on the surface of graphite with electrolytes is somewhat more than that of without electrolytes. It is reasonable to expect that additional collector adsorbed on the graphite surface will improve the hydrophobicity of graphite. Besides, the peak at 473.46 cm^{-1} was caused by $-\text{SH}$, and the antisymmetric stretching vibration of $-\text{CH}_2$ was shown at $2925\pm 5\text{ cm}^{-1}$ (Kumar et al, 2002; Xia et al, 2017). The peaks at 3416.72 cm^{-1} and 3619 cm^{-1} are associated with the $-\text{OH}$ of hydrogen bonded alcohols and phenols (Wang et al., 2016). Alcohol hydroxyl and phenolic hydroxyl, hydrophilic oxygenated functional groups have been suggested for the formation of more stable hydrated film on the surface of mineral, which greatly reduced the floatability of mineral (Sen and Srivastava, 2009; Qu, 2015). Furthermore, $-\text{NH}$, $-\text{NH}_2$ and $-\text{OH}$ of alcohols and phenols were detected at about 3416.72 cm^{-1} . There was no significant difference between the intensity of the $-\text{NH}$, $-\text{NH}_2$ and $-\text{OH}$ bands for the sample conditioned in the absence and presence of MgCl_2 . It can be seen clearly from the whole spectra that no new absorption peaks were detected in the presence of MgCl_2 , which indicated it was only physical adsorption in the presence of Mg^{2+} .

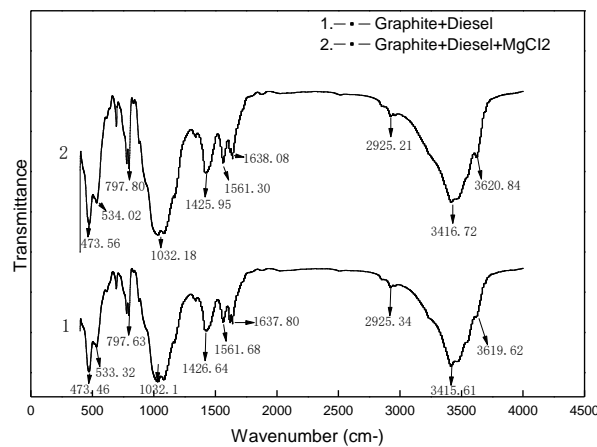


Fig. 5. FTIR spectrogram of graphite sample conditioned with collector (Diesel) in the presence and absence of the MgCl_2

3.6 Surface tension experiments

Diesel oil was selected as the collector. Remaining diesel oil after the adsorption with graphite gathered at the interface between gas and liquid, due to the lower density, insolubility of diesel in water and the surface power. As the Gibbs isotherm adsorption equation shown:

$$\Gamma = \frac{-c}{RT} \frac{dr}{dc} \quad (2)$$

where Γ is the adsorption capacity at the interface between gas and liquid, c is the equilibrium concentration of diesel in liquid, R is gas constant, T is the absolute temperature, dr/dc is the surface activity of diesel (The ability of diesel reduced surface tension.). Γ is closed with the gas-liquid surface tension. In pulp, the concentration of diesel decreases with the increasing adsorption capacity of graphite when the input of diesel remains constant. Therefore, the surface tension of gas-liquid interface changes with the adsorption capacity of graphite at the constant conditions.

As shown in Fig. 6, the addition of MgCl_2 increased the surface tension of gas-liquid interface. This means that the free diesel in the pulp decreases with the increasing concentration of MgCl_2 . In other words, there are more collector adsorbed on the mineral surface, which contribute to the floatability of graphite. The significant increase in the collector adsorption is probably due to the reduction in the magnitude of electrostatic attraction between graphite and gismondine at the present of MgCl_2 . Since a great amount of fresh surfaces of graphite was produced due to the desorption of gismondine in weak electrostatic field, the hydrophobicity of graphite was greatly improved. The result is well consistent with other studies reported by Cebeci (2002) and Dey (2012). As the decreasing wettability of the coal, it is easy for common oily collectors to spread across the coal surface. In the study of Ozdemir et al

(2009), contact angle did not change in the presence of salt ions without the addition of collector. It is noted that the improvement of wettability was not attributable to the electrolyte itself. And, collectors and electrolytes play a synergistic role in flotation process.

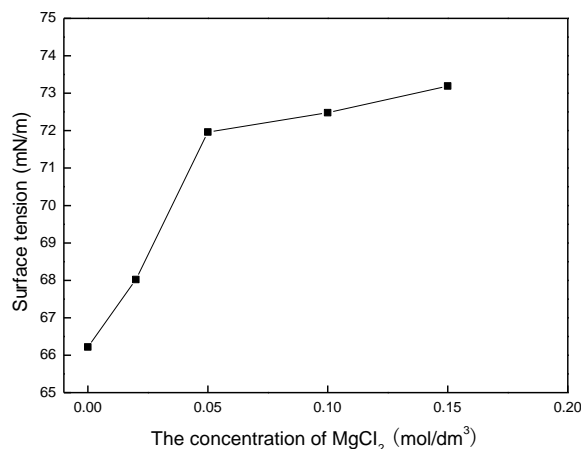


Fig. 6. Effect of electrolytes concentration on surface tension of gas-liquid interface

4. Conclusions

The recovery of graphite could be enhanced from 85.62 to 91.26% using diesel collector in the presence of MgSO₄. Besides, the fixed carbon content of concentrate increased by about 1%. This was probably due to the weakened detrimental electrostatic attraction between graphite and gismondine and the reduction of entrainment in flotation process. The potential of mineral was reduced dramatically due to the stern layer adsorption and compression of electric double layer. Therefore, the electrostatic attraction between graphite and gismondine was weakened, which be beneficial to the full dispersion of minerals. Dispersed graphite particles with less impurities contamination on its surface have better hydrophobicity, which contributes the spreading of oil collectors on the surface of particles.

Acknowledgments

This research was supported by the Natural Science Foundation of Jiangsu Province (BK20150192). The authors also acknowledge the assistance of Project Funded by the Priority Academic Program Development of Jiangsu Higher Education Institutions.

References

- PAULSON O., PUGH R.J., 1996, *Flotation of inherently hydrophobic particles in aqueous solutions of inorganic electrolytes*, *Langmuir*, 12(20), 4808-4813.
- GRAIG V.S.J., NINHAM B.W., PASHLEY R.M., 1993, *The effect of electrolytes on bubble coalescence in water*, *Journal of Physical Chemistry*, 97(39), 10192-10197.
- CASTRO S., LASKOWSKI J.S., 2011, *Froth flotation in saline water*, *Powder & Particle*, 29(29), 4-15.
- CHOI J., CHOI S.Q., PARK K., HAN Y., KIM H., 2016, *Flotation behaviour of malachite in mono- and di-valent salt solutions using sodium oleate as a collector*, *International Journal of Mineral Processing*, 146, 38-45.
- CHEN X., PENG Y., 2015, *The effect of regrind mills on the separation of chalcopyrite from pyrite in cleaner flotation*, *Minerals Engineering*, 83, 33-43.
- CRUNDWELL F.K., 2016, *On the mechanism of the flotation of oxides and silicates*, *Minerals Engineering*, 95, 185-196.
- CEBECI Y., 2002, *The investigation of the floatability improvement of yozgat ayridam lignite using various collectors*, *Fuel*, 81(3), 281-289.
- DICKSON A.G., GOYET C., 1994, *Handbook of Methods for the Analysis of the Various Parameters of the Carbon Dioxide System in Sea Wate*, Version 2. Oak Ridge National Lab., TN, United States.
- DEY S., 2012, *Enhancement in hydrophobicity of low rank coal by surfactants – a critical overview*, *Fuel Processing Technology*, 94(1), 151-158.

- GUI X., XING Y., RONG G., CAO Y., LIU J., 2016, *Interaction forces between coal and kaolinite particles measured by atomic force microscopy*, Powder Technology, 301, 349-355.
- HIRAJIMA T., SUYANTARA G.P.W., ICHIKAWA O., ELMAHDY A.M., MIKI H., SASAKI K., 2016, *Effect of Mg²⁺, and Ca²⁺, as divalent seawater cations on the floatability of molybdenite and chalcopyrite*, Minerals Engineering, 96-97, 83-93.
- HANCER M., CELIK M.S., MILLER J.D., 2001, *The significance of interfacial water structure in soluble salt flotation systems*, Journal of Colloid & Interface Science, 235(1), 150.
- KLASSEN V.I., MOKROUSOV V.A., 1963, *An Introduction to the Theory of Flotation*, Butterworths, London.
- KUMAR T.V., PRABHAKAR S., RAJU G.B., 2002, *Adsorption of oleic acid at sillimanite/water interface*, Journal of Colloid & Interface Science, 247(2), 275.
- LAGALY G., ZIESMER S., 2003, *Colloid chemistry of clay minerals: the coagulation of montmorillonite dispersions*, Advances in Colloid & Interface Science, 100(02), 105-128.
- LIANG Y., HILAL N., LANGSTON P., STAROV V., 2007, *Interaction forces between colloidal particles in liquid: theory and experiment*, Advances in Colloid & Interface Science, 134-135(21), 151.
- LI C., SOMASUNDARAN P., 1991, *Reversal of bubble charge in multivalent inorganic salt solutions-Effect of magnesium*, Journal of Colloid and Interface Science, 146(1), 215-218.
- LEE H.T., NEETHLING S.J., CILLIERS J.J., 2005, *Particle and liquid dispersion in foams*, Colloids & Surfaces A Physicochemical & Engineering Aspects, 263(1):320-329.
- RATTANAKAWIN C., HOGG R., 2000, *Aggregate size distributions in flocculation*, Songklanakarin Journal of Science & Technology, 177(2-3), 87-98.
- LIU D., PENG Y., 2014, *Reducing the entrainment of clay minerals in flotation using tap and saline water*, Powder Technology, 253(2), 216-222.
- MANONO M.S., CORIN K.C., WIESE J.G., 2012, *An investigation into the effect of various ions and their ionic strength on the flotation performance of a platinum bearing ore from the merensky reef*, Minerals Engineering, 36-38(36-38), 231-236.
- MANONO M.S., CORIN K.C., WIESE J.G., 2016, *The influence of electrolytes present in process water on the flotation behaviour of a cu-ni containing ore*, Minerals Engineering, 96-97, 99-107.
- MISHCHUK N., 2005, *The role of hydrophobicity and dissolved gases in nonequilibrium surface phenomena*, Colloids Surf., A 267, 139-152.
- OATS W.J., OZDEMIR O., NGUYEN A.V., 2010, *Effect of mechanical and chemical clay removals by hydrocyclone and dispersants on coal flotation*, Minerals Engineering, 23(5), 413-419.
- OZDEMIR O., 2013, *Specific ion effect of chloride salts on collectorless flotation of coal*, Physicochemical Problems of Mineral Processing, 49, 511-524.
- OZDEMIR, O., TARAN, E., HAMPTON, M.A., KARAKASHEV, S.I., NGUYEN, A.V., 2009, *Surface chemistry aspects of coal flotation in bore water*, International Journal of Mineral Processing, 92(3-4), 177-183.
- PEASE J.D., CURRY D.C., YOUNG M.F., 2006, *Designing flotation circuits for high fines recovery*, Minerals Engineering, 19(6), 831-840.
- PENG Y., BRADSHAW D., 2012, *Mechanisms for the improved flotation of ultrafine pentlandite and its separation from lizardite in saline water*, Minerals Engineering, 36-38, 284-290.
- PAN L., YOON R.H., 2016, *Measurement of hydrophobic forces in thin liquid films of water between bubbles and xanthate-treated gold surfaces*, Minerals Engineering, 98, 240-250.
- QU J., 2015, *Research on Reactive Oily Bubble Flotation Behavior of Low Rank Coal and Its Flotation Technique*, China University of Mining and Technology, 1, 44-125.
- RATH R., LASKOWSKI J., SUBRAMANIAN S., 1999, *Interaction of guar gum with hydrophobic solids*, Canadian Institute of Mining Metallurgy and Petroleum, Canadian.
- SEN R., SRIVASTAVA S. K., MOHAN M., 2009, *Aerial oxidation of coal-analytical methods, instrumental techniques and test methods: a survey*, Indian Journal of Chemical Technology, 16(2), 377-379.
- WANG B., PENG Y., VINK S., 2014, *Effect of saline water on the flotation of fine and coarse coal particles in the presence of clay minerals*, Minerals Engineering, 66-68, 145-151.
- WANG Y., PENG Y., NICHOLSON T., LAUTEN R.A., 2016, *The role of cations in copper flotation in the presence of bentonite*, Minerals Engineering, 96-97, 108-112.
- WANG H., FENG Q., LIU K., 2016, *The dissolution behavior and mechanism of kaolinite in alkali-acid leaching process*, Applied Clay Science, 132-133, 273-280.

- XING Y., GUI X., LEI P., PINCHASIK B.E., CAO Y., LIU J., 2017, *Recent experimental advances for understanding bubble-particle attachment in flotation*, *Advances in Colloid & Interface Science*, 246, 105-132.
- XIA W., ZHOU C., PENG Y., 2017, *Enhancing flotation cleaning of intruded coal dry-ground with heavy oil*, *Journal of Cleaner Production*, 161, 591-597.
- ZHANG X.H., DUCKER W., 2007, *Formation of interfacial nanodroplets through changes in solvent quality*, *Langmuir* 23, 12478-12480.
- ZHAO, S., PENG, Y., 2012, *The oxidation of copper sulfide minerals during grinding and their interactions with clay particles*, *Powder Technology*, 230, 112-117.
- ZHAO S., GUO B., PENG Y., MAI Y., 2016, *An impedance spectroscopy study on the mitigation of clay slime coatings on chalcocite by electrolytes*, *Minerals Engineering*, 101, 40-46.